



ELSEVIER

Journal of Chromatography A, 679 (1994) 231–245

JOURNAL OF  
CHROMATOGRAPHY A

## Column efficiency and radial homogeneity in liquid chromatography

Tivadar Farkas, James Q. Chambers, Georges Guiochon\*

*Department of Chemistry, University of Tennessee, 575 Buehler Hall, Knoxville, TN 37996-1503, USA  
Division of Analytical Chemistry, Oak Ridge National Laboratory, Oak Ridge, TN, USA*

Received 16 March 1994

### Abstract

Local, on-column electrochemical detection was carried out in the amperometric mode at different points of the column outlet cross-section. This permitted the determination of the spatial distribution of analyte molecules within the chromatographic zone at the column exit. The radial distribution of the peak-maximum velocity, the local efficiency and the analyte concentration were determined for a commercial column and for several laboratory-packed columns made with different solid particles and with a commercial silica-based stationary phase. An important region of the packing close to the wall is denser, has a lower permeability and a lower efficiency than the core of the packing. The concentration along the wall is lower than average, in part because of the lower efficiency.

### 1. Introduction

In the entire chromatography literature, with only very few exceptions [1–5], most of them nearly twenty years old, columns are seen as unidimensional. This means that their radial homogeneity is assumed to be sufficiently high on the scale of the column radius for minor radial fluctuations of the packing density not to cause any problems. The analyte bands are assumed to exhibit a constant concentration over the entire column cross-section. Similarly, if a preparative column is overloaded, the degree of overload, or loading factor, is assumed to be constant in the radial direction. There is little experimental evidence in support of these assumptions, except for the feeling, not entirely unjustified, that should it be otherwise, column

performance would be drastically decreased compared to what is routinely achieved.

In the early development stage of high-performance liquid chromatography, Knox and co-workers [1,2] showed that packed columns are not radially homogeneous, but that there is a wall region, extending to ca. 30 particle diameters from the wall, which is less homogeneous than the column core. If the column is sufficiently wide in relation to its diameter and to the particle size, the molecules of a sample injected in the center of the column would not have time to reach the wall region before they elute. Thus, the zone would move in a highly homogeneous packing and the column performance would be as good as if the wall region did not exist and the packing was entirely homogeneous. By contrast, if a sufficient proportion of the molecules in a zone can reach the wall region and experience the dispersive effect of this different and less

\* Corresponding author.

homogeneous part of the packing, the apparent column efficiency drops markedly [2]. Knox and co-workers [1,2] recommended the use of columns having a diameter in excess of four standard deviations of the radial dispersion. For all practical purposes, these columns would be equivalent to "infinite diameter columns" [1].

The technological developments of liquid chromatography have made this approach practically impossible to follow. Conventional 1/4 in. O.D. (1 in. = 2.54 cm) columns are somewhat long and narrow, making marginal the achievement of the infinite column diameter condition. A 250 × 4.6 mm column packed with 10- $\mu\text{m}$  particles has to be operated at a reduced velocity,  $\nu$ , in excess of 5 ( $\nu$  should exceed 20 with  $d_p = 20 \mu\text{m}$ , 2 with  $d_p = 5 \mu\text{m}$ ) to satisfy the infinite diameter column condition [2]. Since these columns are usually operated at reduced velocities of around 8 in most analytical applications, the condition would be satisfied provided the injection is made at the very column center and the diameter of the injected pulse is very small. However, syringe injection has been universally replaced by valve injection. The sample band is carried into the column by the mobile phase stream which flushes the content of the sample loop. This makes it impossible to perform an axial injection. On the contrary, the injection pulse is spread over the entire column cross-section area. Similarly, in preparative chromatography injection is made by switching, for a given period of time, the sample solution for the mobile phase as the pump feed. The use of valve injection is not compatible with the operation of any column under the "infinite diameter column" mode.

Later, Eon [3] studied radial dispersion in chromatographic columns. He showed that radial dispersion proceeds at a slower pace than axial dispersion. This is in agreement with the results of Knox et al. [2] and with the general results derived from thin-layer chromatography [6]. However, his careful measurements demonstrated that, as a larger and larger fraction of the sample penetrates into the wall region, the column height equivalent to a theoretical plate

(HETP) appears to increase with increasing column length instead of remaining constant, which is a basic tenet of the theory of linear chromatography. This fact may explain various inconsistencies found in the literature regarding the plate height equations and, in Eon's opinion, casts some serious doubts regarding the validity of the conclusions of many publications made in this area [3]. Finally, Eon [3] showed that radial compression improves markedly column performance, presumably because it reduces the density difference between the wall region and the column core.

Recently, Baur et al. [4] have investigated the radial distribution of analyte molecules in chromatographic bands by means of electrochemical detection in the amperometric mode, using carbon fiber electrodes placed close behind the column outlet frit. They found that the radial distribution of the analyte concentration across narrow analytical columns (ca. 3.2 mm I.D.) was surprisingly uneven, although valve injection was used which obviously should prevent the achievement of an axial injection. The retention time is a few percents larger along the wall than in the center. They also showed that the coefficient of axial dispersion and the column efficiency depends strongly on the radial position. The reduced plate height may be four times as large along the wall than in the center part of the column. The radial concentration profiles measured were used to reconstruct the band profiles recorded with a bulk detector. This work demonstrates that at least a large part of the residual tailing observed in cases where there can be little polar interaction between solutes and stationary phase is due to the wall effects.

In spite of their clarity and importance, these results have not yet been assimilated in the culture of chromatographers. For the last twenty years, analysts have generally assumed that wall effects are negligible in analytical columns. It seems strange to them that any significant fluctuations of the packing density may arise over distances as short as the column radius, cause an uneven radial distribution of the concentration of analytes, and have major effects on the column

efficiency. The packing material does look homogeneous, and unpacking columns does not show any difference between core and wall regions. Finally, it is not easy to detect the effects shown by Knox and co-workers [1,2], Eon [3] and Baur et al. [4]. Conventional detectors determine the cross-section average concentration of the mobile phase and are useless for the purpose. Knox et al. [2] and Eon [3] used a dual polarographic detector for their experimental studies. This is not an easy technique. Injections have to be repeated many times since the chromatogram in one single point of the column cross-section can be recorded. Finally, and most importantly, the range of column efficiencies currently achieved seems satisfactory to most users.

The problem of column homogeneity is becoming relevant again, however. There is growing evidence that preparative columns are at least moderately inhomogeneous [7,8] and should be considered as two-dimensional packed beds, i.e., cylindrical, rather than one-dimensional ones, i.e., linear. Recent modeling studies have shown that the long-range fluctuation of the mobile phase velocity in a radially compressed preparative column may exceed 5%, but does not probably reach 10%, except in really bad situations [5]. In conventional packed columns, voids are known to appear at the top of the column after some period of time. This formation is blamed on the lack of "wall support" of the packing [9]. It is certainly due, at least in most part, to a progressive settling of the packing particles, accompanied by a decrease in the column porosity [7–9]. The cause of this phenomenon, and the factors which influence its kinetics are unknown at present. The packing homogeneity and stability of preparative columns needs systematic investigations [8].

Because even the packing structure of analytical columns is still poorly known and understood, it seems interesting to investigate it again in this context. In this first paper, we report on the results of systematic measurements of the radial distribution of the mobile phase velocity and the radial shape of the elution band of a

compound on various analytical columns by means of on-column electrochemical detection. Simultaneous measurements were carried out at different locations.

## 2. Experimental

### 2.1. Detection device

Conventional detectors measure the cross-section average composition of the eluent at column outlet. The distribution of the analyte molecules along the column axis is classical. The determination of the radial distribution requires local, on-column determination of the concentration of the eluent at different points of the cross-sectional area, allowing for mapping the analyte distribution over this area before all molecules reunite in the effluent, heading then for the post-column bulk detector.

Like Baur et al. [4], we used electrochemical detection in the amperometric mode, with gold electrodes rather than carbon fiber electrodes placed close behind the column outlet frit. The gold microelectrodes were prepared by inserting a 50- $\mu\text{m}$  nominal diameter gold wire into a 25–30 mm long section of fused-silica capillary tubing 150  $\mu\text{m}$  I.D. (Polymicro Technologies, Phoenix, AZ, USA). The space between the gold wire and the inner wall of the tube was filled with an epoxy resin (Epon Resin 828; Shell, Houston, TX, USA). The tips of the electrodes were polished with diamond paste (sizes 1 then 1/4). The other end of the gold wire was connected to a copper conductor by means of a silver epoxy connection (Epo-tek H20E; Epoxy Technology, Billerica, MA, USA), insulated with the same epoxy resin. Cyclic voltammograms were run with a BAS 100 electrochemical analyzer (Bioanalytical Systems, West Lafayette, IN, USA) in order to assess for the actual area of the electrodes.

To avoid obvious electrical problems, the electrodes were inserted in holes drilled into a non-metallic frit (Upchurch Scientific, Oak Harbor, WA, USA) placed at the outlet end of the

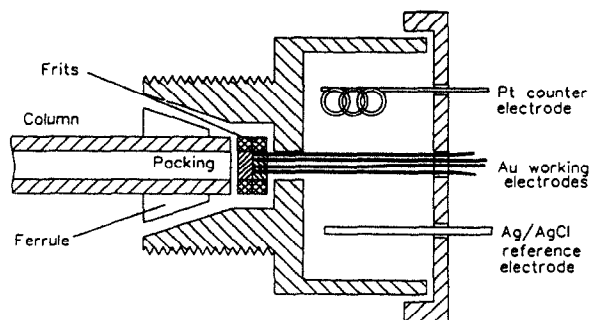


Fig. 1. Schematic of the detector arrangement for four gold working electrodes, a platinum counter electrode and a reference electrode.

chromatographic column. Four electrode tips are placed at different radial positions, facing a second, identical frit placed against the column packing and holding it when the external frit is rotated to permit the acquisition of other sets of data (Fig. 1). One electrode is placed near the center of the frit, two other electrodes are at almost equal distance from the axis, at about  $r_c/2$  ( $r_c$  = column radius), in perpendicular directions, and a fourth electrode is close to the wall (Fig. 2). In order to acquire more data points over the column cross-section area, each experi-

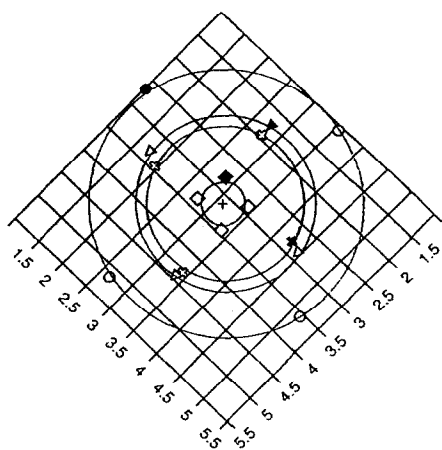


Fig. 2. Position of the electrodes at the column end (solid symbols) and successive positions during a measurement cycle (solid and open symbols).

ment was done four times, and the frit was rotated by  $90^\circ$  steps around the column axis between successive experiments. Thus, 16 data points are collected in each case. The electrode positions are shown in Fig. 2, with the four solid black symbols corresponding to the points collected at one position of the frit.

The aspect of the polished electrode surface was investigated under microscope. All four electrode tips protruding slightly from the frit could be brought together into focus under a high-resolution microscope. Thus, the four electrode tips were in the same plane perpendicular to the column axis. The outlet fitting of the column was modified in order to allow for a four-electrode set-up, for the amperometric detection of electroactive compounds. A platinum counter electrode, and an Ag/AgCl reference electrode were placed behind the outlet frit in the cup-shaped fitting (Fig. 1). The output of each electrode was amplified by means of a Voltammograph Model CV-37 (Bioanalytical Systems). Systematic electrode fouling was experienced. The electrode tips were cleaned before each experimental run by means of sweeping the applied potential from  $-1$  to  $+1$  V (electrolytic polishing).

## 2.2. Liquid chromatography equipment

The chromatographic system consisted of a Waters (Milford, MA, USA) HPLC Pump Model 510, a Spectraflow Model 575 absorbance detector (Applied Biosystems, Ramsey, NJ, USA) as the bulk detector, when needed, and a Rheodyne (Cotati CA, USA) HPLC injection valve Model 7010. The data of either the UV detector or the four electrochemical detectors were acquired using a Waters system interface module with two A/D convertor boards permitting the simultaneous monitoring of four detectors. Waters Maxima 820 version 3.3 software was used to collect the data at a rate of 10 data points per second. The data files were uploaded to one of the computers of the University of Tennessee Computer Center for further calculations.

### 2.3. Injection profile

The shape of the injection profile has a critical importance in this work. Significant spacial deviations of the profile of the injected plug of sample from the shape of a rectangular band propagating under piston flow conditions would affect the elution profile as much as the lack of radial homogeneity in the column packing that we try to investigate. It is important to determine the possible contribution of the injection profile to our results. The problem of the influence of the design and operating conditions of the injection device on the band profile has been lucidly discussed by Kirkland et al. [10]. Only the considerable improvements made during the last twenty years to the chromatographic equipment have affected the conclusions of this work. Modern columns are closed with a low porosity frit which is tightly crimped at the column inlet. A distributor is placed on the top of the column, above the frit. This provides a relatively flat profile for the front of the injection band when it reaches the column inlet. Because of the parabolic profile of the flow velocity across an empty tube such as the sample loop, the rear of the injection profile tends to assume also a parabolic shape. The use of a narrow, coiled capillary tube as sample loop enhances the radial diffusion in this tube by triggering a secondary circulation. This contributes to alleviate the curved rear of the injection profile.

Measurements of the electrode responses to the injection of samples in a column of length  $L=0$ , obtained by putting the assembly of electrodes described later directly against an inlet frit and a distributor has given results showing an almost flat injection band, although its axial profile is far from rectangular. Fig. 3 shows typical injection profiles recorded under the same conditions as those used for the chromatograms discussed later in this report and obtained with real columns having 15 to 25 cm in length. The sample concentration rises and decays slightly more slowly along the column wall than in its center. However, there is little difference between the maxima of the two profiles and the delay between the maxima of the profiles

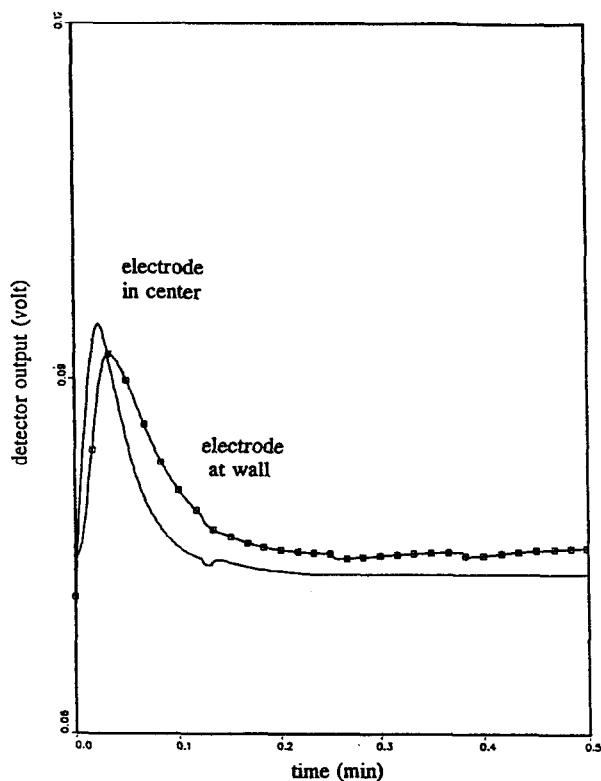


Fig. 3. Injection profiles recorded without column, using the center and wall electrodes.

recorded at the column center (first arrived) and along the column wall is of the order of 0.5 s only, to be compared with values of the order of 12 s observed at the column exit between the retention times of the corresponding profiles at the column center and along its wall.

This demonstrates that the results reported below are due essentially to phenomena taking place inside the column. The contribution of the equipment and, more specifically, of the injection device to these results is essentially negligible.

### 2.4. Chromatographic columns

Most of the investigated columns ( $200 \times 4.6$  mm) were packed in the laboratory with commercially available packing materials;  $40\text{-}\mu\text{m}$  glass beads (EM Separations, Gibbstown, NJ,

USA), 10- and 16- $\mu\text{m}$  porous silica and  $\text{C}_{18}$ -silica (PQ Corp., now BTR Separation, Wilmington, DE, USA) were used. A Kromasil (Eka Nobel, Bohus, Sweden) KR10-16- $\text{C}_{18}$  column packed by the manufacturer was also studied.

### 2.5. Chromatographic mobile phase

A 0.1 M KCl aqueous electrolyte solution was used as the mobile phase, except for the reversed-phase columns packed with  $\text{C}_{18}$  silica. Since this material is poorly wet by water [11], 20% methanol was added to the mobile phase. This concentration was chosen because it was the highest for which the amperometric detector worked satisfactorily. It was insufficient, however, to achieve good efficiencies with the reversed-phase column. Fig. 4 shows a conventional plot of the reduced height equivalent to a theoretical plate for benzoquinone (see next section) on this column as a function of the

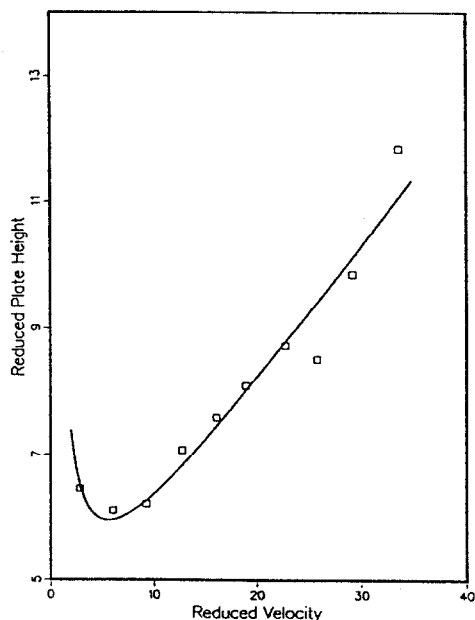


Fig. 4. Plot of the reduced plate height versus the reduced velocity for the Kromasil KR100-16- $\text{C}_{18}$  column. Column dimensions,  $100 \times 4.6$  mm; particle size, 16  $\mu\text{m}$ ; mobile phase, methanol–0.1 M aqueous KCl (20:80). Sample, benzoquinone, 0.1 M solution.

reduced velocity. The data in Fig. 4 were obtained with the UV detector, measuring the column efficiency from the concentration profile in the bulk stream of mobile phase. A value nearly half as large was observed for the minimum plate height with the same column and compound but a water–methanol (40:60) solution as the mobile phase. This suggests that this commercial column is well packed.

The use of a saline, water-rich solution as eluent of a silica column guarantees low or negligible retention factors for most analytes. This is not a problem in the present work, as we study the hydrodynamic properties of the packed bed. Their effects on band profiles is expected to be independent of the possible retention, and to contribute to the total band width following the rule of variance additivity [12]. The influence on the analyte retention of local fluctuations of the stationary phase density will be studied separately.

### 2.6. Samples

As explained above, the effect studied is clearer on a non-retained peak. Sensitive detection is not an issue either. The samples were chosen to optimize the behavior of the amperometric detector. Several compounds, potassium ferricyanide, hydroquinone and benzoquinone could easily be detected electrochemically under conditions satisfactory for our purpose. However, the electrolyte mobile phase is corrosive and dissolved enough  $\text{Fe}^{2+}$  from the stainless-steel column wall to cause rapid fouling and clogging of the column and exit frit by deposition of Prussian Blue. This ruled out the use of the ferricyanide/ferrocyanide redox couple.

Dilute solutions of benzoquinone in the electrolyte solution used as the mobile phase proved to be much more stable than the too readily oxidizable hydroquinone solutions. Because of the poor solubility of benzoquinone in electrolyte solution used as mobile phase,  $1 \cdot 10^{-3}$  to  $1 \cdot 10^{-4}$  M solutions were used. The applied potential difference between the working electrode and the reference electrode for optimum

benzoquinone detection was  $-0.45$  V. Samples of  $20 \mu\text{l}$  were injected for each experiment.

## 2.7. Calibration

Calibration proved to be the most difficult task of this work. It was only partly successful, as we were able to measure only the relative concentrations of the tracer. In order to calculate the local concentration of analyte from the value of the current drawn during the experiment, the response factor for each microelectrode has to be determined. Cyclic voltammograms were run as mentioned previously, and from the value of the resulting limiting current, the actual area of the electrode could be calculated. This parameter cannot be used in the calibration for two reasons.

First, the gold surface of the electrode proved to be highly sensitive to electrochemical fouling that could not be entirely removed by rinsing or ultrasonication. This fouling reduces the active area of the electrode, hence diminishes the response factor. Thus, a frequent, systematic electrochemical cleaning is necessary. However, each cycle of electrolytic polishing removes also a thin metal layer from the fresh gold surface that could not be removed and later small pieces of epoxy insulation around the electrode tip. As a consequence, the active area of the electrode increases in time. These two phenomena have opposite effects. Overall, we found that the limiting current increased significantly during the first week of using the electrode, and then decreased gradually to very small values due to irreversible surface deactivation. The cyclic voltammograms run before using the electrode, and after one week of usage are shown in Fig. 5, demonstrating the effects of an initial increase of the active electrode area, followed by electrochemical fouling of the electrode tip.

The electrode response factor could not be determined by elution experiments because, although the initial concentration of the injected sample is known, the local, actual concentration at the electrode tip is unknown as a consequence of the radial distribution of analyte concentration

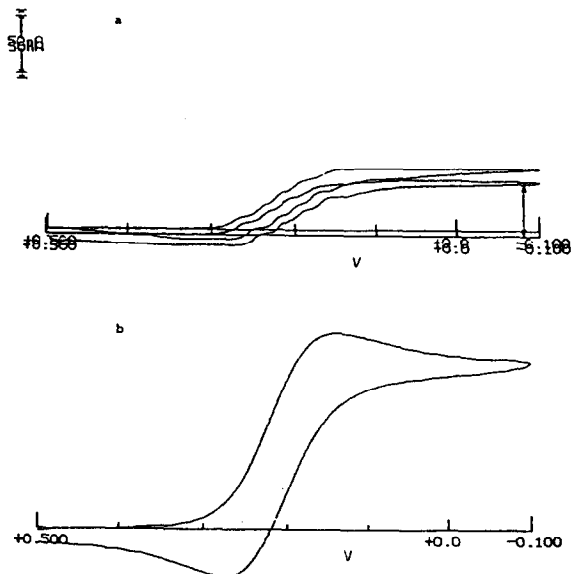


Fig. 5. Cyclic voltammograms run (a) with the electrodes in their initial clean state; (b) after 1 week of experiments. Solution,  $0.05$  M benzoquinone in  $0.1$  M KCl. Scan rate,  $20$  mV/s.

within the component zone. Recalculating the actual electrode area after every short series of experiments by running cyclic voltammograms under steady-state conditions is not practical because of the poor mechanical resistance of the electrodes.

Frontal analysis provides the only practical solution. In this case, the four electrodes are measuring the concentration of the same solution when the plateau at the injection concentration has been reached. This permits the calibration of each electrode relative to the others at the beginning and end of each such experiment. However, the method is quite time consuming, and the extent to which it can be used is limited by fouling, so only a small number of calibration points can be acquired. Accordingly, it was carried out only in connection with the measurements made for the determination of the radial distribution of the analyte concentration. Other experiments were performed without relating the signals of the individual electrodes to the solute concentration.

## 2.8. Procedures and reproducibility

Each experiment consists in the injection of a small, known amount of benzoquinone as a dilute solution, and the recording of the four electrode signals. The experiment is repeated a number of times, with rotation of the electrode holder by an angle of  $90^\circ$  between successive determinations.

The repeatability of the experiment is assessed periodically by performing series of injections without intermediate rotations, with successive rotations of  $360^\circ$  angles, and with successive rotations of  $90^\circ$  angles. The first series of such experiments gives the repeatability of the injection and detection systems. The results of one such experiment are reported in Fig. 6a. The profiles obtained are identical. The slight shift between the successive signals is due to fluctuations in the delay between the manual actuation of the injection valve and the data acquisition device. Table 1 shows the reproducibility of the differences between the retention times measured with two different electrodes (6 different pairs). Since the two electrodes at  $r_c/2$  from the column center are at  $90^\circ$  angle, the difference between their peak maxima is small and less reproducible than for the other five pairs.

The second series of experiments includes the contribution of the additional error made in repositioning the electrodes. Typical results are given in Fig. 6b which shows essentially the same degree of repeatability. The results of the third series of experiments are illustrated in Fig. 6c, as plots of the difference between the retention times measured from the signal of the central electrode and from each of the three other electrodes. The repeatability of the signal of the central electrode is the same as in Fig. 6b, and its fluctuations are due to errors in the timing of the initial data point. This error does not affect the differences shown in Fig. 6c. The repeatability of this difference under the conditions of Fig. 6a is 0.005 min. The fluctuations seen in Fig. 6c, especially at the wall, demonstrate that the velocity distribution is not exactly cylindrical. Obviously, the fluctuations of the retention time observed across the column exceeds largely the errors of measurements.

## 3. Results and discussion

### 3.1. Radial distribution of the mobile phase velocity

It would be difficult and meaningless to measure the velocity in any given point of the column. This velocity is chaotic, not only in space, but also in time, because of the eddies which form between particles. The velocity varies rapidly and considerably from the wall of a particle to the center of each interparticle channel. Some averaging is necessary. The cross-section averaged velocity,  $u = L/t_0$ , is widely used to characterize the convective transport along the column. To study the packing homogeneity we need to average the velocity over a distance which is short compared to the column diameter, but large compared to the particle size. The electrode diameter ( $50 \mu\text{m}$ ) is barely larger than the coarser particles used in this work ( $40 \mu\text{m}$ ), but the electrode is placed in a silica sleeve ( $150 \mu\text{m}$ ) which causes the formation of a local eddy, hence averaging on a space scale of the order of a few particle diameters, which seems to be sufficient. In the plots presented here we give the relative difference,  $(u - \bar{u})/\bar{u}$ , between this local average velocity and the cross-section averaged velocity,  $\bar{u} = L/t_0$ .

In an homogeneously packed tube, the radial profile of the velocity averaged over a few particle diameters should be essentially constant, from the axis to the wall. The effect of a lower packing density at the very wall, because particles cannot penetrate into a smooth wall, would be averaged out if the velocity measured is an average calculated over a few particle diameters. The classical Poiseuille parabolic velocity profile applies to empty tubes, to some extent to the interparticle channels (which have too small an aspect ratio for this law to apply strictly), but not to packed columns. Experimental results, however, deviate from this ideal model of the velocity profile.

The plots in Figs. 7a–d show the results obtained for the distribution of the mobile phase velocity in the different columns studied. Fig. 7a shows a three-dimensional plot of the velocity versus the position of the electrodes in the 40-



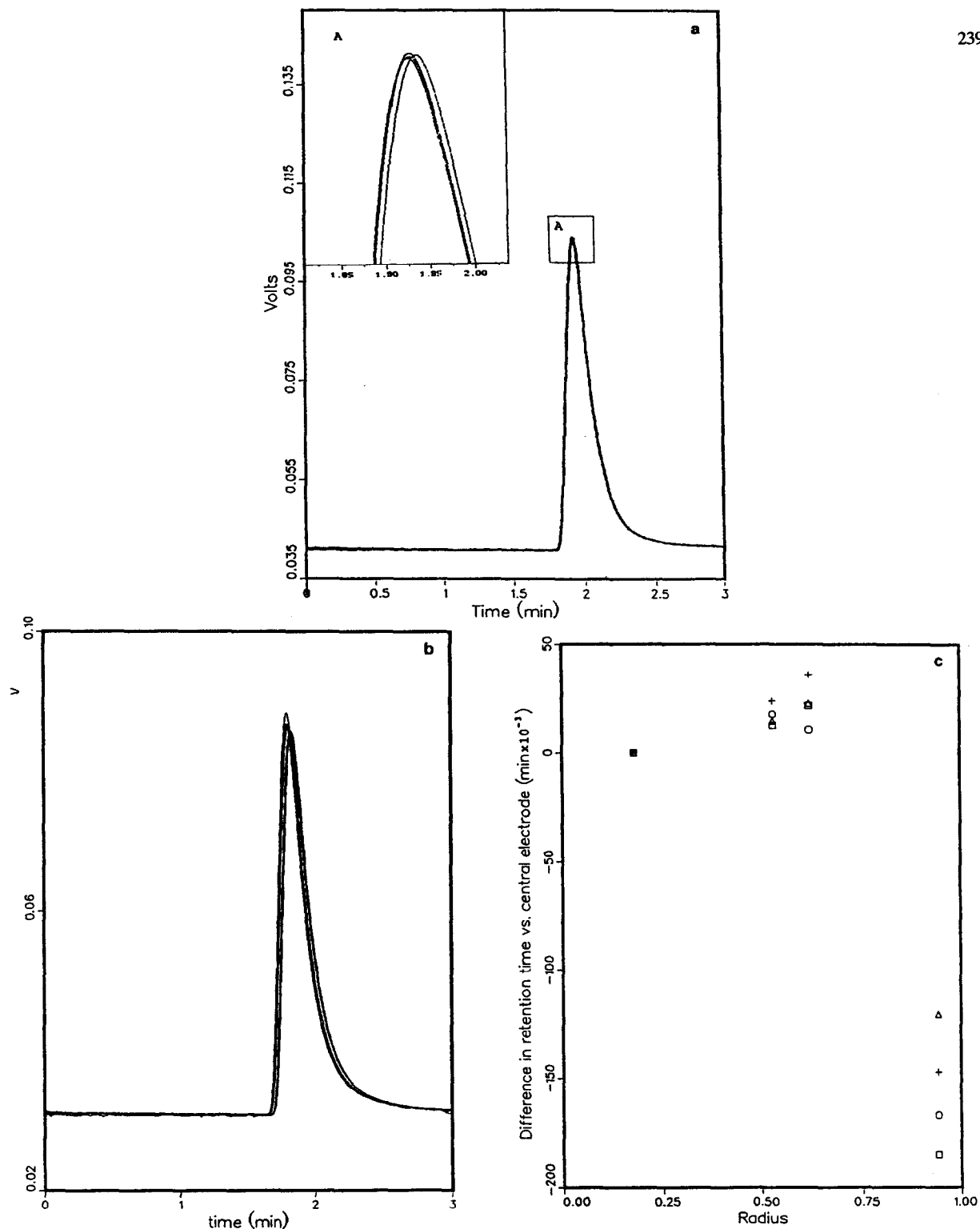


Fig. 6. Reproducibility of the measurements. (a) Four successive chromatograms obtained with the central electrode, without moving the electrode assembly between successive measurements, overlaid. (b) As (a), but the electrode assembly is rotated one full turn between two successive measurements. (c) Differences between the retention times measured by the central electrode and any of the other three electrodes at four different positions ( $0^\circ$ ,  $90^\circ$ ,  $180^\circ$  and  $270^\circ$ ) of the electrode assembly. "Radius" indicates relative radius,  $r/r_c$ .

Table 1  
Reproducibility of retention time differences

Electrode pair <sup>a</sup>	$\Delta t_R$ (s)	$\sigma$ (s)	$\sigma/t_R$ (%)
C-W	7.23	0.53	7.2
C-M1	2.10	0.10	2.8
C-M2	3.90	0.25	6.5
M1-M2	1.15	0.36	32
M1-W	10.5	0.48	4.6
M2-W	7.80	0.40	5.0

The injections were done without moving the electrodes between successive injections. Average and relative standard deviation ( $\sigma/t_R$ ) of 8 experimental results.

<sup>a</sup> C = Center electrode; M1 = electrode at  $r_c/2$ , in the plane of C and W; M2 = other electrode at  $r_c/2$ ; W = electrode at the wall (see Fig. 2).

$\mu\text{m}$  glass bead column. It is obvious that the mobile phase velocity is systematically lower close to the wall than in the center of the column. There is a high velocity ridge about half-way through the column, where the velocity is maximum. This ridge is more clearly visible in Fig. 7b, which is a projection of the data in Fig. 7a on the  $z, y$  plane of Fig. 7a. The velocity is nearly constant over a core section of the packing which has a diameter of nearly a third of the column inner diameter. The diameter of the ridge is equal to approximately two third of the column diameter.

The phenomenon is unambiguous. The time differences observed are important, much larger than the experimental errors, as shown in the section on reproducibility (see Figs. 6a–c). For example, the delay between the elution of the fastest peak (electrodes half way from the center to the wall) and the slowest peak (along the wall) is of the order of 14 s (12% of  $t_R$ ), while the band width at half-height of these peaks does not exceed 10 s, and the standard deviation on the retention time of a peak is between 0.1 and 0.5 s, depending on experimental conditions (table or figure).

The glass bead column was unpacked, then repacked twice. The new results are shown in Fig. 7c, as a plot of the relative velocity differences versus the radial position of the electrode

for all measurements made on these columns. This plot shows that the velocity distribution is highly repeatable, except, may be, at the very wall, where angular fluctuations do exit (Fig. 7c). This result demonstrates that the packing method used provides column beds which are highly reproducible, even though they are not ideal. Finally, Fig. 7d compares the results obtained with one of the 40- $\mu\text{m}$  glass bead columns, and a 10- $\mu\text{m}$  silica particle column also packed by us. The radial distributions obtained are nearly identical, although the retention factor of benzoquinone in this case was different from 0 ( $k' = 0.22$ ). This shows that the phenomenon observed does not strongly depends on the solute retention, as expected from its hydrodynamic nature.

This phenomenon was not observed by Knox et al., who report “little [radial] variation of peak-maximum velocity” [2, summary] for an 11 mm I.D. column, but still a 4% *higher* velocity at the wall than at the center [2, Fig. 6b]. Eon [3] obtained similar results with two 17 mm I.D. columns, one made of steel, the other of PTFE (for radial compression). The velocity near the wall is 3 to 4% *higher* than in the column center. In neither case is there any velocity ridge around the column core region. Results similar to ours were reported by Baur et al. [4] who used a 3.2 mm I.D. column, and found that the retention time increases by a few percents close to the wall (2% at 0.2 mm from the wall, i.e., at 65 particle diameters). In our columns, the thickness of the wall region seems to be ca. 15% of the column diameter, or 30 particle diameters, a figure in excellent agreement with the values reported by Knox et al. [2] and by Eon [3] for the thickness of the wall region in their columns. Opposite to these authors’ findings, however, and in agreement with Baur et al., we observe that the velocity is lower at the wall, by up to 12%, and not higher.

### 3.2. Radial distribution of the column efficiency

For the sake of providing proper reference, we have shown in Fig. 4 the conventional plots of the reduced column efficiency versus the reduced mobile phase velocity, as measured with the UV

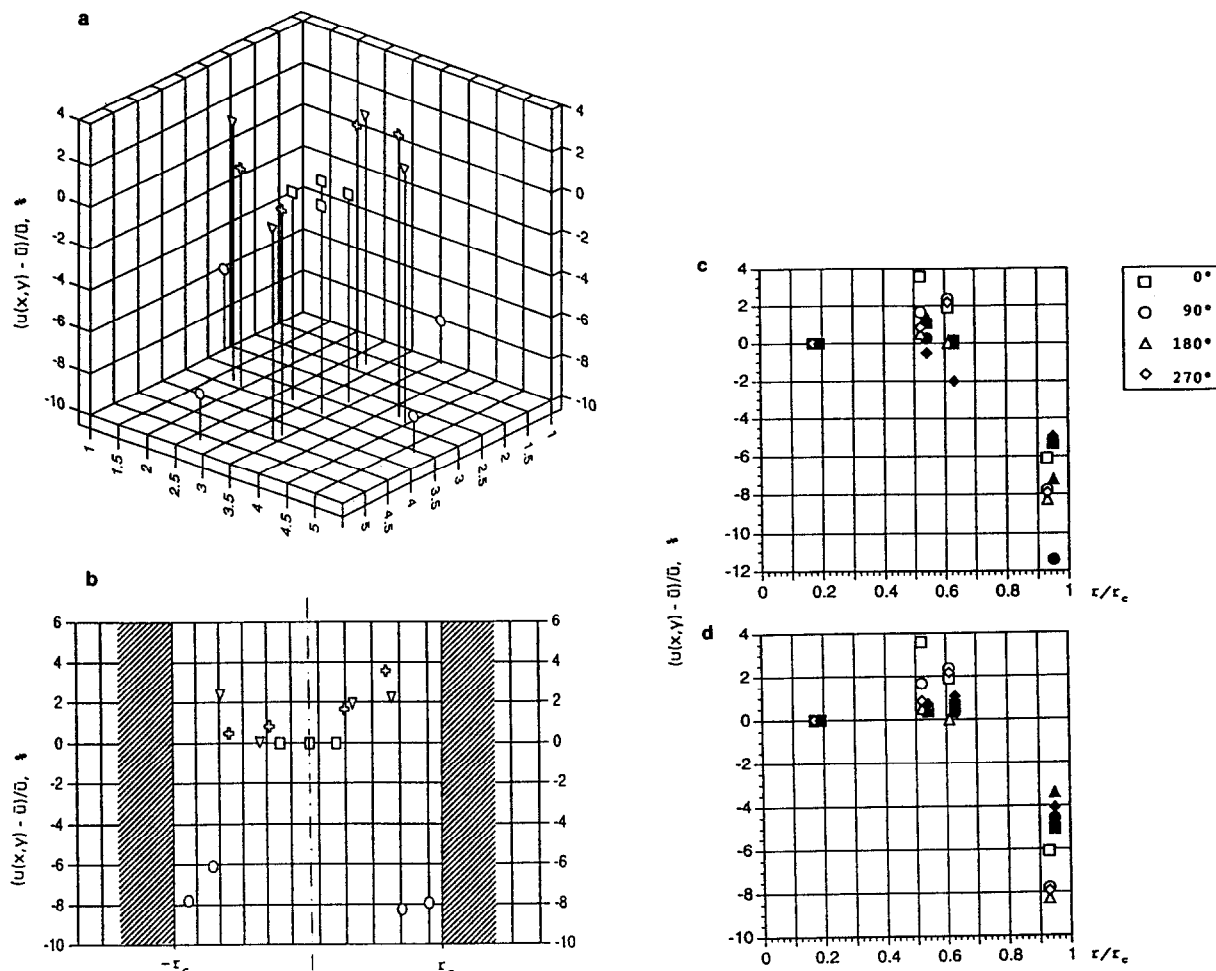


Fig. 7. Plot of the relative velocity difference,  $[u(x,y) - \bar{u}]/\bar{u}$ , versus the position of the electrode. (a) False three-dimensional plot of the relative velocity difference versus the coordinates of the electrode at the column exit. Column packed with 40- $\mu\text{m}$  glass beads. (b) Projection of the three-dimensional plot in (a) on the  $y,z$  plane. Figs. 7a and b, symbols as in Fig. 2. (c) Plot of the relative velocity difference between the radial distance of the electrode. Data obtained with two different columns packed with the same 40- $\mu\text{m}$  glass beads, overlaid. (d) Plot of the relative velocity difference between the radial distance of the electrode. Data obtained with one column packed 40- $\mu\text{m}$  glass beads and with one column packed with 10- $\mu\text{m}$  porous silica particles, overlaid.

detector for the commercial column. As benzoquinone is practically not retained on any of the columns, the slope of the curve at high reduced velocities is essentially due to mass transfer resistances in the mobile phase. It is smaller for glass bead columns than for conventional silica columns, as the beads are not porous. Note, however, that because of its definition, the cross-sectional average velocity depends on the internal porosity of the particles. For a given flow-

rate, the hold-up time is approximately twice as large for a porous silica particle (with total porosity = 0.8) as for non-porous glass beads, hence  $\bar{u}$  is twice smaller, while the actual values of the solvent velocities around the particles are the same.

The width recorded for an elution band depends considerably on the position of the electrode. As seen in the Figs. 8a–c, the column efficiency calculated from the width of the band

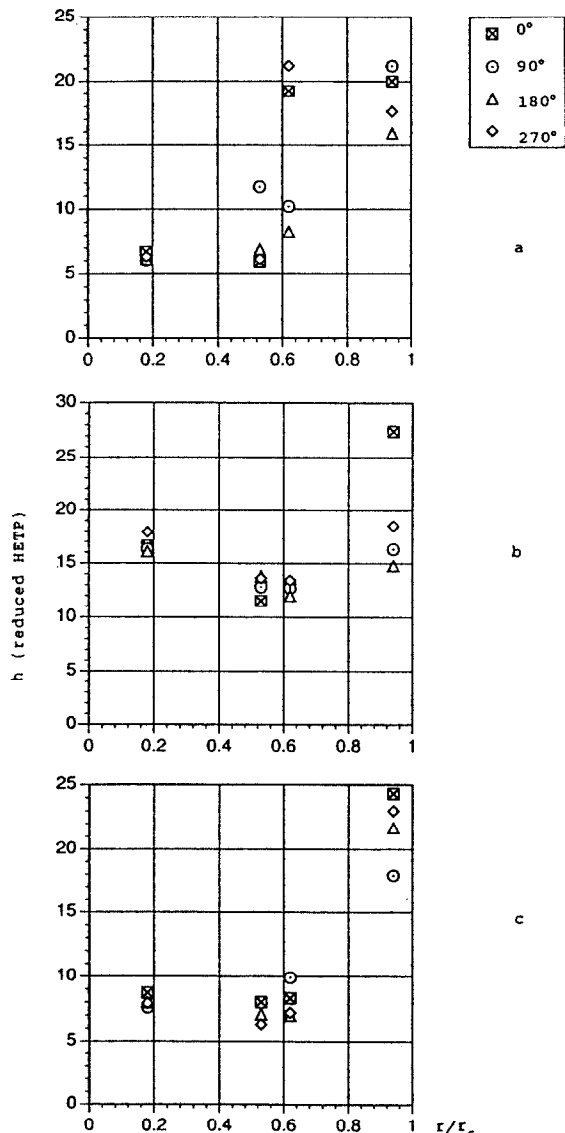


Fig. 8. Plot of the column reduced HETP versus the radial position of the electrode tip. (a) Column packed with 40- $\mu\text{m}$  glass beads. (b) Column packed with 10- $\mu\text{m}$  porous silica particles. (c) Kromasil column, 10 cm long, packed with 16- $\mu\text{m}$  porous particles of octadecyl silica.

at half-height depends much upon the radial position of the electrode. However, the results obtained with the different columns show more variability for the efficiency than for the mobile phase velocity distribution.

Fig. 8a illustrates the dependence of the ef-

iciency on the electrode position in the exit cross-section for the column packed with 40- $\mu\text{m}$  glass beads. The most efficient section of this column seems to involve the core and the intermediate region corresponding to the velocity ridge. Within this center, most of the data points are around 900 theoretical plates, corresponding to a reduced plate height of ca. 5.5 (for a reduced velocity of ca. 90). However, some data points in this region can be as low as 300 plates, which is very poor, and unexpected. The efficiency drops sharply in the region close to the column wall, where all the data points are below 350 plates. Furthermore, peaks recorded at radial positions close to the wall show strongly distorted and wide band shapes. Examples are shown in Fig. 9.

Fig. 8b shows a plot of the column HETP versus the radial position of the electrode for the column packed with 10- $\mu\text{m}$  particles. The result is quite similar, but with the notable difference of a clear maximum at the velocity ridge, where the efficiency is nearly three times larger than along the wall, against 2.5 times in the center. As in the other column (Fig. 8a), the efficiency drop is precipitous around two-thirds of the distance between the center and the wall. As seen in both Fig. 8a and b, it seems that the column is not exactly cylindrical, but that the "wall region" is thicker along some directions than along others.

As seen in Fig. 8c, the commercial column, packed with 16- $\mu\text{m}$  particles, seems to be somewhat more homogeneous than our packed columns, although the results are substantially the same. The shape of the plot of the column efficiency versus the radial position is quite similar to those seen in Fig. 8b, and to that of the plot of the peak-maximum velocity versus the radius (Fig. 7d). The column efficiency is poor at the column wall, maximum along the velocity ridge, and lower at the center. However, the efficiency drop observed near the column wall is much less important than in the other columns. The efficiency at the wall is about 60% of the maximum, along the velocity ridge, and, quite surprisingly, more than 90% of the efficiency in the core region. This column is

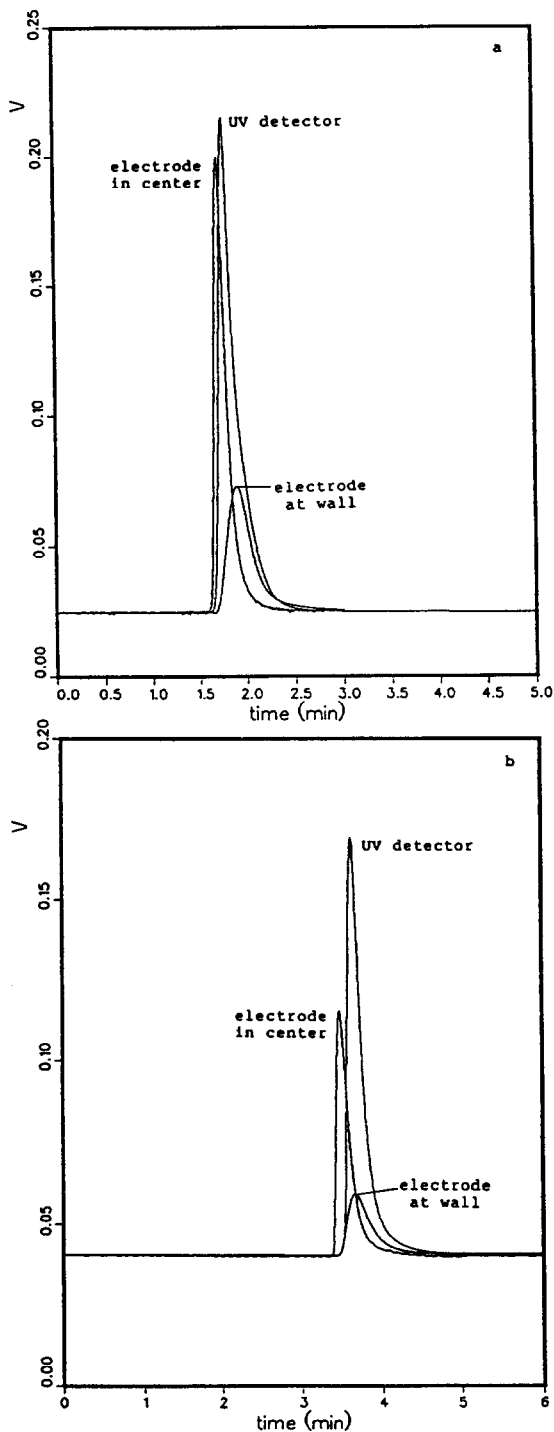


Fig. 9. Comparison between chromatograms recorded with the central and the wall electrodes. (a) Column packed with 40- $\mu\text{m}$  glass beads. (b) Column packed with 10- $\mu\text{m}$  porous silica particles.

certainly much more homogeneously packed than those made in our laboratory.

These results agree with those previously published, but only to a point. As reported here, Knox et al. [2], Eon [3], and Baur et al. [4] found that the column efficiency is much better at the center than along the wall. The profiles of the radial distribution of the column efficiency shown by Knox and co-workers [2], by Eon [3] and by Baur et al. [4] are similar to those shown in Fig. 8. In all these cases and in the present work, the maximum efficiency is two to three times higher than the efficiency near the wall. However, all these authors found the column efficiency to be constant in the central core region. This is not the case for the different columns studied here, even for the commercial column. This shows that more work is necessary to develop an improved packing technology which could reduce or eliminate the wall region and give a more homogeneous, more efficient packed bed.

A consequence of the experimental results of previous authors, confirmed by our own results, is that markedly better separations could be performed by HPLC if only on-column detection were used. A three-fold gain in column efficiency is a major achievement, translating into a 70% better resolution, or three times faster analyses. If this approach is used, however, the positioning of the detecting sensor should be carefully chosen, inside the core area within half a column radius from the column axis, or better, along the velocity ridge.

### 3.3. Radial distribution of analyte concentration

Fig. 10a shows the distribution of the signal maximum over the column cross-section corrected for the differences in response compared to the electrode placed close to the column axis. Despite the relative lack of precision in the determination of the local concentrations at different values of the column radius, we see that the maximum concentration of the peaks is largest at the column center and in the core region, while it is three to four times lower along the column wall.

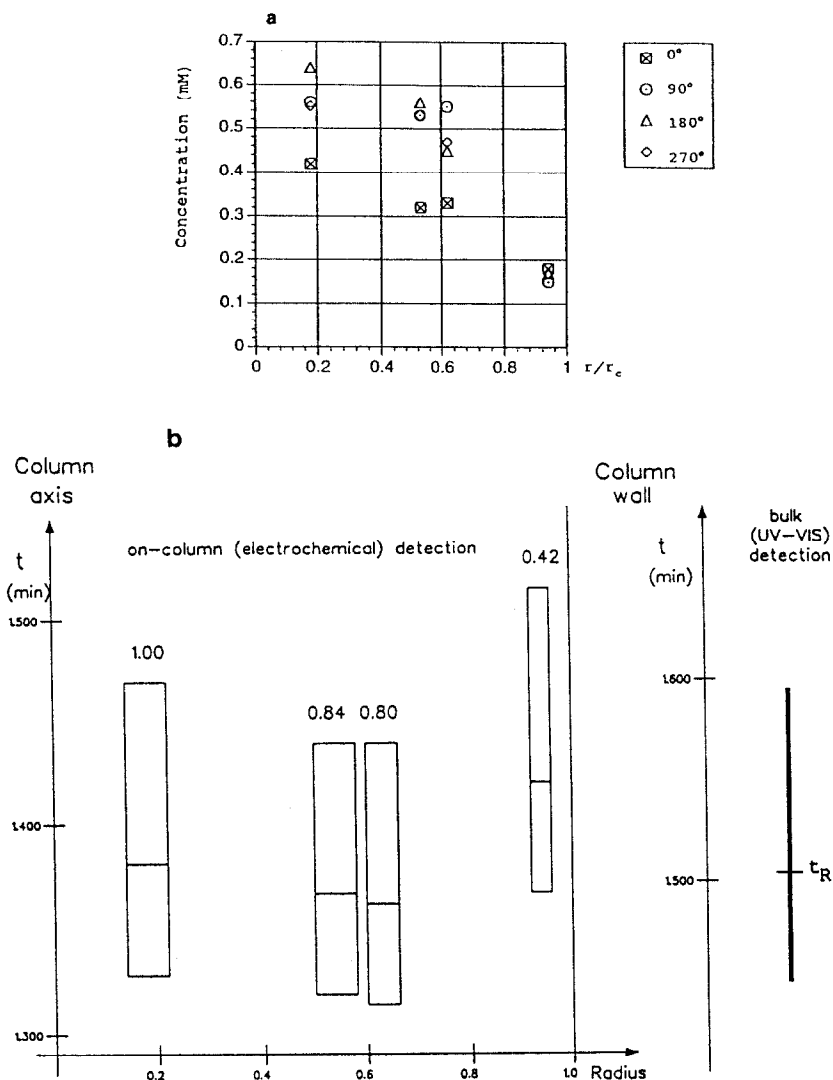


Fig. 10. Radial distribution of the concentration and amount of solute in the column. (a) Maximum concentration of the chromatograms. Kromasil column. (b) Amount of material accounted for by the chromatogram. Abscissa: radial position, as  $r/r_c$ .

This result is in agreement with our previous findings. Since the bands are wider and the column efficiency is poorer at the wall than in the core region, the same amount of material injected per unit surface area will give a peak shorter along the wall than in the center. However, multiplying the peak height and its width at half-height gives a figure which is proportional to the peak area. This value is not constant across the column, but increases, albeit much less

rapidly than the peak height, from the column wall to its center (Fig. 10b). This latter finding explains why the large peak width recorded at the column wall does not contribute more to the overall peak width observed with a bulk detector. The results shown in Fig. 10a are in excellent agreement with those of Baur et al. [4]. The ratio of the maximum peak concentrations at the column center and along its wall is ca. 5 in their case, about 3 to 4 in ours.

As shown in the Experimental section, it is possible to rule out any significant contribution of the injection band profile to the radial distribution of the solute concentration. The principle, design and mode of operation of the sampling valve and its connection to the column permit the achievement of almost flat injection profiles. Because the concentration profile of an analyte along the wall passes later and is wider and shorter than in the column center, the signal of a bulk detector is bound to exhibit some degree of tailing, even if the peak profile at any point of the column cross-section is Gaussian. This phenomenon could provide a likely explanation to the puzzling tailing exhibited by weakly polar or non-polar compounds on well-deactivated, end-capped, carefully bonded octadecyl silica packings.

#### 4. Conclusions

Although the details of our results are different from those obtained by previous workers [1–4], there is a substantial agreement regarding the nature of the phenomenon. Analytical HPLC columns are not radially homogeneous. On the contrary, a rather homogeneous core is surrounded by a thick layer of packing along the wall. The thickness of this layer is around 30 to 50 particle diameters. Why this layer is sometimes less permeable and probably denser than the core, as in our experiments and those of Baur et al. [4], while in other cases it is more permeable, as in the experiments of Knox and co-workers [1,2] and Eon [3], and why this is so, remains open for discussion. This observation is important as it does not seem to be consistent with the conventional explanation regarding the low stability of the beds in preparative columns, that these beds are lacking “wall support”. The wall region contributes more to band broadening than the core region. Band profiles recorded at the column wall are later eluted, more dilute and

wider than those recorded in the center during the same experiment.

As a consequence, analytical columns are operated under experimental conditions where a significant fraction of their potential performance is wasted. A small concentration sensor placed at the column axis would see narrower, better resolved and more concentrated bands. Recent progress in the realization of microelectrodes and optical fibers could permit the design of improved chromatographs. The fact that the analyte is more concentrated in the areas where the efficiency is higher renders this approach more attractive.

The behavior of packed column beds and the dynamics of the packing methods are still poorly understood [7–9]. Further progress in the performance of analytical as well as preparative columns could be expected from research done in these areas.

#### References

- [1] J.H. Knox and J.F. Parcher, *Anal. Chem.*, 41 (1969) 1599.
- [2] J.H. Knox, G.R. Laird and P.A. Raven, *J. Chromatogr.*, 122 (1976) 129.
- [3] C.H. Eon, *J. Chromatogr.*, 149 (1978) 29.
- [4] J.E. Baur, E.W. Kristensen and R.M. Wightman, *Anal. Chem.*, 60 (1988) 2338.
- [5] T. Yun and G. Guiochon, *J. Chromatogr. A*, 672 (1994) 1.
- [6] F. Geiss, *Fundamentals of Thin Layer Chromatography*, Hüthig, Heidelberg, 1987.
- [7] M. Sarker and G. Guiochon, *LC·GC*, 12 (1994) 300.
- [8] M. Sarker and G. Guiochon, *J. Chromatogr. A*, in press.
- [9] H. Colin, in G. Ganetsos and P.E. Barker (Editors), *Preparative and Production Scale Chromatography*, Marcel Dekker, New York, 1992, p. 47.
- [10] J.J. Kirkland, W.W. Yau, H.J. Stoklosa and C.H. Dilks, Jr., *J. Chromatogr. Sci.*, 15 (1977) 303.
- [11] G. Körösi, A.M. Siouffi and G. Guiochon, *J. Chromatogr. Sci.*, 18 (1980) 324.
- [12] J.C. Sternberg, *Adv. Chromatogr.*, 2 (1966) 205.